POLITECNICO DI TORINO
Repository ISTITUZIONALE

Fatigue assessment of a new concept for a floating barge with pendulum for offshore wind turbines in MOST

(Article begins on next page)

31 December 2024

PAPER • OPEN ACCESS

Fatigue assessment of a new concept for a floating barge with pendulum for offshore wind turbines in MOST

View the article online for updates and enhancements.

Fatigue assessment of a new concept for a floating barge with pendulum for offshore wind turbines in MOST

Massimo Sirigu, Alberto Ghigo, Ermando Petracca, Giuseppe Giorgi, Giovanni Bracco

Marine Offshore Renewable Energy Lab, Politecnico di Torino, Corso Duca degli Abruzzi 24, Torino, 10129, Italy

massimo.sirigu@polito.it, alberto.ghigo@polito.it, ermando.petracca@polito.it, giuseppe.giorgi@polito.it, giovanni.bracco@polito.it

Abstract. Among floating foundations for offshore wind turbines, the barge is considered one of the most cost-effective platforms, owing to its ease of manufacturing, transport, and installation. However, the barge platform is susceptible to wave-induced stress due to its extensive waterplane area, potentially leading to fatigue in critical structural components such as the platform, tower, nacelle components and moorings. This paper delves into the prospect of mitigating fatigue damage in the barge concept by introducing a pendulum ballast, which can be installed at the offshore site using polyester ropes. The primary focus of this research is the assessment of the 'barge-pendulum' concept, aimed at reducing load cycles that could lead to fatigue failure, with a specific emphasis on the tower base as a representative indicator of device damage. The analysis is conducted using MOST, a time-domain simulation code developed in Matlab-Simscape environment. The findings show that the barge-pendulum concept has a poorer performance in terms of fatigue life, due to the increased sensitivity to wave forces.

1. Introduction

The increasing global demand for sustainable energy sources has driven remarkable growth in offshore wind energy production. Harnessing the abundant and consistent wind resources offered by the world's oceans presents a significant opportunity to transition towards a cleaner and more sustainable energy landscape. Offshore wind turbines (OWT), with its potential as a renewable energy source due to higher wind speeds and larger available areas, present a promising alternative to onshore wind. However, the challenge lies in its relatively high costs. In contrast to the mature onshore wind technology, offshore wind technology faces greater challenges due to demanding operating conditions and increased costs. OWT experience higher structural loads than their land-based counterparts. Typically, offshore wind turbines are deployed near the coastline, where water depths are less than 60 meters, making fixed-bottom foundations economically viable. But as we venture into deeper waters, the need for floating support structures becomes apparent, and this shift poses a significant challenge for industrialization. Opportunities for cost reduction include strategies such as reducing platform size and weight, optimizing mooring systems and anchors, and enhancing installation and maintenance processes.

Within the industry, three major platform types are commonly utilised: buoyancy-stabilised (semi-submersible, barge), mooring-stabilised (tension-leg platform), and ballast-stabilised (spar buoy) [1].

Emerging innovative designs that blend various substructure principles are increasingly gaining attention. Hexafloat [2] showcases an innovative hexagonal framework tethered to a central ballast

through six ropes. In addition, the industry has witnessed the introduction of the TetraSpar, a creation of Stiesdal, and a damping pool barge, a concept patented by Ideol [3]. The TetraSpar's design stands out for its use of a tubular steel framework and a keel that hangs beneath it. The idea behind the TetraSpar is to use components that are already well-established in industrial manufacturing, making it easier to build and scale up [4]. Ideol's barge design features a unique moonpool intended to modify the platform's natural frequency as per the patent's concept [5].

The barge is recognized as one of the most cost-effective alternatives in offshore platforms, mainly due to its straightforward manufacturing, transportation, and installation processes. However, the barge platform is susceptible to wave-induced stress due to its extensive waterplane area and higher natural frequencies, potentially leading to fatigue in critical structural components such as the platform, tower, nacelle components and moorings. To address this, we'll explore a strategy to reduce fatigue damage in the barge design by introducing a magnetite or concrete ballast or pendulum. The purpose of the pendulum is to lower natural frequencies and nacelle acceleration thanks to a higher pitch inertia and obtain the same static pitch angle with small dimension of the platform, reducing excitation forces on the body. The pendulum can be installed at the offshore site using a set of polyester ropes. The primary focus is the assessment of the barge-pendulum concept, aimed at reducing load cycles that could lead to fatigue failure, with a specific emphasis on the tower base as a key indicator of device damage. Additionally, this work includes the analysis of the barge-only platform for comparison purposes, evaluating differences in mass and tower fatigue.

Finally, we'll look at differences in size and how each design affects different properties, like static pitch angle, natural frequencies, effect of waves, ultimate loads, and finally fatigue on tower base, providing a comprehensive understanding of the benefits and limitations.

2. Methodology

The turbine under consideration is the IEA 15 MW wind turbine [6], while the properties of the tower are taken from [7], more suitable for the floating condition. The control system is based on the ROSCO (Reference Open-Source COntroller) [8]. It employs standard wind industry control strategies like tip speed ratio (TSR) tracking and gain-scheduled PI control for generator torque and blade pitch, but also incorporates advanced functions such as a feedback-based nacelle velocity control loop and thrust peak shaving to limit maximum thrust near the rated wind speed, albeit with an energy production trade-off.

To facilitate a comprehensive evaluation and enhancement of the two concepts, named barge-only and barge-pendulum platform (figure 1), we use a systematic evaluation procedure. This evaluation process is organized into three fundamental steps for each of the concepts.
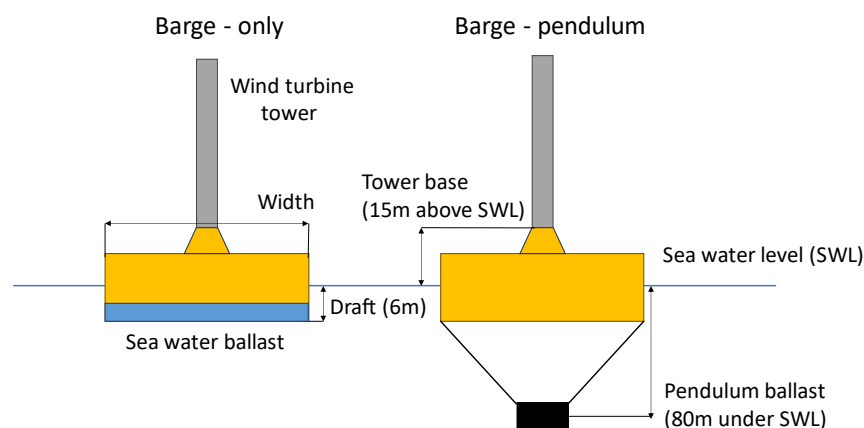

Figure 1. illustration of the two concepts.

In the initial step, the focus is on assessing the hydrostatic parameters, such as the platform mass, centre of gravity, submerged volume, and the determination of the required ballast mass to achieve static equilibrium. The second step is the frequency domain analysis, intended to analyse the natural frequency and the wave induced nacelle acceleration. The third step is a time-domain analysis.

We conduct a time domain analysis using MOST, a Matlab-Simscape model capable of simulating the complex multibody dynamics of the pendulum [9]. In this analysis, we treat the pendulum as a separate body, connected to the main platform by means of four ropes, each of which is modelled as a linear spring. The platform's geometry is modelled using Salome [10], an open-source software capable of generating three-dimensional geometry based on predefined parameters. The geometry is imported into Nemoh [11], enabling the extraction of linear hydrodynamic properties such as added mass, radiation damping, and excitation forces.

2.1. Hydrostatic analysis

The hydrostatic analysis involves the computation of the mass, inertia, and the necessary ballast to achieve the desired draft.

The variables under consideration are the platform's width W and draft D. The computation of the mass, centre of mass and moment of inertia is carried out using Salome 9.9.0 [12]. The external and internal geometry is shown in figure (2). for all surfaces, the thickness is set at 2 cm. The material employed is structural steel, which has a density of 7850 kg m^{-3}.

The net mass M_{Net} required to maintain the design draft is evaluated in equation (1), Where ρ is the density of sea water (1025 kg m^{-3}), V_s is the submerged volume, $M_{turbine}$ is the mass of the wind turbine, including tower, rotor and nacelle assembly (2425 ton) and M_{steel} is the structural mass of the platform, $F_{moorpreload}$ is the mooring preload divided by the gravity acceleration.

$$M_{Net} = \rho \cdot V_s - M_{steel} - M_{turbine} - \frac{F_{moorpreload}}{g} \tag{1}$$

To calculate the centre of mass and inertia of the internal water ballast for the barge-only configuration, it is assumed that the ballast is fully enclosed within the barge, beginning from the platform's base, and mass of ballast is equal to M_{Net}. To determine the final mass of the pendulum ballast, considering its submersion in seawater, the additional buoyancy provided by the body requires an increase in mass.

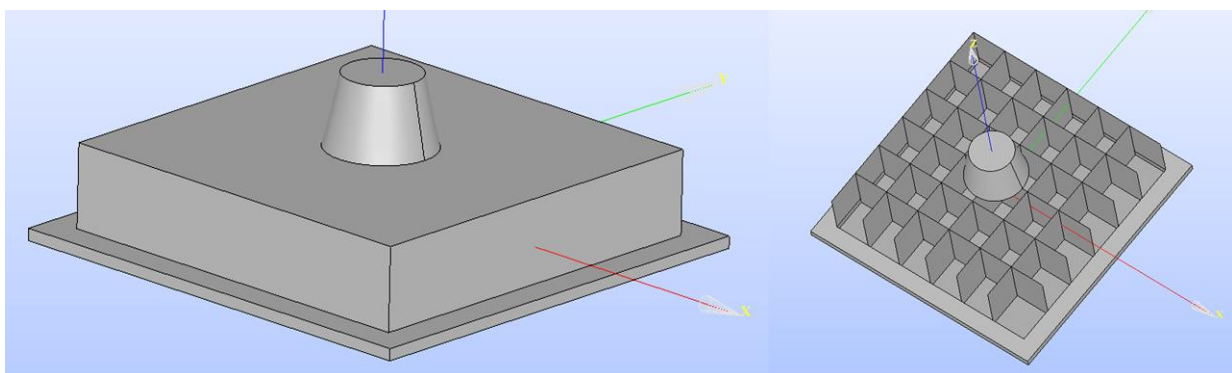**Figure 2.** Representation of external and internal geometry of the barge in Salome 9.9.0. The skirt width is 4 meters beyond the barge's width and 1 metre height, 5 internal stiffeners are located internally, located as squared grid, and a transition piece, modelled as a cone, is placed to connect the barge to the tower base. All elements are modelled as surfaces with thickness 2 centimetres.

This concept can be expressed as follows:

$$M_{Pendulumballast} = \frac{\rho_{ballast}}{(\rho_{ballast} - \rho_{water})} M_{Net} \tag{2}$$

The ballast may be built using either magnetite, which has a density of 5170 kg/m³, or concrete, with a density of 2400 kg/m³. A comparative analysis will be conducted between these two types of ballast, focusing on their respective impacts on total inertia and drag.

This study adopts mooring line characteristics akin to those of the Volturn US platform [7], with minor deviations. Four lines are attached to the platform's extremities, and the linear mass is reduced to 565 kg/m. The fairlead is connected to the platform's corners at its bottom and is dependent on the platform's dimensions (table 1). The mooring lines are catenary (steel chains).

To maintain consistency in mooring stiffness compared to the reference model, adjustments are made to the anchor depth and radial distance, ensuring the same horizontal and vertical distances relative to the fairlead. The mooring line tension is modelled using the catenary equation. The mooring forces are then applied to the body's reference system.

Table 1. Definition of mooring lines in function of platform geometry. D is the draft; W is the width.

Number of Lines	(-)	4	Fairlead Radial Spacing	(m)	$W/\sqrt{2}$
Dry line linear mass	(kg)	565	Anchor radial spacing	(m)	$779.6 + W/\sqrt{2}$
Anchor depth	(m)	$186 + D$	Fairlead Depth	(m)	D
Extensional Stiffness	(MN)	3270	Line Unstretched Length	(m)	850

2.2. Pendulum analysis

The pendulum is modelled as a six degrees of freedom body using the library of Simscape Multibody; the ballast is connected to the main body by means of four ropes, connected to the corner of the platform, modelled as linear springs. In our work, the height of the pendulum is equal to the radius and the mass and volume are evaluated in equation (1). The values for minimum breaking load and stiffness for different materials are taken from Orcaflex database [13], [14]. Polyester rope is chosen in this study, because it has an intermediate stiffness value between nylon and wire ropes. The load design, compared with minimum breaking load ($170466 \, d^2$) is equal to the net mass of the pendulum (ballast mass minus buoyancy) divided by the number of ropes, with a safety factor of 2.5. Once obtained the diameter dimension, the spring stiffness is computed using the axial stiffness of the material ($1.09 \times 10^6 \, d^2$).

2.3. frequency domain analysis

The hydrodynamic analysis involves the computation of the response amplitude operator $\xi(w)$ (RAO), the device's pitch resonance period T and root-mean-square (RMS) of the nacelle acceleration due to wave response $NacAcc_{RMS}$, shown respectively in equation (3), (4) and (5), where w is the frequency (rad/s), and h_{hub} is the hub position respect to SWL (150 m). The mesh created in Salome is imported in Nemoh 3.0 to evaluate the added mass A, radiation damping B and excitation forces F_{ext}, M is the pitch inertia of the platform and turbine combined. In this context, JONSWAP spectrum $S_{JP}(w)$ is employed to determine the unidirectional irregular sea state condition, as implemented in WecSIM [15].

$$\xi(w) = \frac{F_{ext}(w)}{-w^2 \left(M + A(w)\right) + iw \, B(w) + K} \tag{3}$$

$$T_{pitch} = \lim_{w \to \infty} 2\pi \sqrt{\frac{M + A(w)}{K}} \tag{4}$$

$$NacAcc_{RMS} = \sqrt{\int_0^\infty \left| w^2 \cdot \xi_{pitch}(w) \cdot h_{hub} \right|^2 S_{JP}(w) \, dw} \tag{5}$$

2.4. Time domain analysis

The time-domain model is implemented in MOST. MOST is a Matlab-simscape model created by Politecnico di Torino [16]. MOST is created to satisfy the needs of a new simulation environment to accommodate for a fast prototyping and proof of new concepts, based on multibody dynamics of platforms. In our work, MOST is needed to evaluate the multibody motion of the pendulum and the main floating structure. The hydrodynamics of the platform is based on the boundary element method (BEM), based on linear hydrodynamics, as implemented in Wec-Sim [17].

The aerodynamics is implemented using blade element momentum theory as described in [18]. The aerodynamic properties of the blade like chord, twist etc. are taken from the distribution of the code in the Github repository [19]. The comparison of the code of MOST with OpenFAST is done in [16].

The resolution of the BEM considers the floating motion of the rotor, by adding the relative velocity of each node of the blade to the wind speed and rotor speed taking into account the motion in six degrees of freedom.

2.4.1. Quadratic drag coefficients

The quadratic drag forces are not included in the boundary element method as the hypotheses are based on the potential flow theory, and the additional formulation is treated separately. To evaluate the drag, the most used formula is to relate the square of the velocity with a constant value, depending on the geometry (equations 6), where ρ_w is the density of the sea water, $\dot{x}_i$ is the velocity of the platform with i the relative degree of freedom, taken relative to the centre of buoyancy, D is the draft and W is the width. The representative area for the rotational degrees of freedom is found by following the equations used in Orcaflex [20]. Although these coefficients are not validated with experimental/CFD data, we assume that they could be representative of the real drag forces experienced by the platform.

$$
\begin{aligned}
F_{drag_1} &= \left(\frac{1}{2} 1.05 \, \rho_w \, W \, D \, |\dot{x}_1| \right) \dot{x}_1 & M_{drag_4} &= \left(\frac{1}{2} 1.05 \, \rho_w \, \frac{W^5}{32} \, |\dot{\omega}_1| \right) \dot{\omega}_1 \\
F_{drag_2} &= \left(\frac{1}{2} 1.05 \, \rho_w \, W \, D \, |\dot{x}_2| \right) \dot{x}_2 & M_{drag_5} &= \left(\frac{1}{2} 1.05 \, \rho_w \, \frac{W^5}{32} \, |\dot{\omega}_2| \right) \dot{\omega}_2 \\
F_{drag_3} &= \left(\frac{1}{2} 1.05 \, \rho_w \, W^2 \, |\dot{x}_3| \right) \dot{x}_3 & M_{drag_6} &= \left(\frac{1}{2} 0.8 \, \rho_w \, \frac{D \, W^4}{16} \, |\dot{\omega}_3| \right) \dot{\omega}_3
\end{aligned}
\tag{6}
$$

The quadratic drag coefficient for the pendulum is proportional to the front area (equation 7).

$$
\begin{aligned}
F_{drag_{surge/sway}} &= \left(\frac{1}{2} 0.6 \, \rho_w \, H_{pend} \, D_{pend} \, |\dot{x}_{1,2}| \right) \dot{x}_{1,2} \\
F_{drag_{heave}} &= \left(\frac{1}{2} 0.6 \, \rho_w \, \frac{1}{4} \pi \, D_{pend}^2 \, |\dot{x}_3| \right) \dot{x}_3
\end{aligned}
\tag{7}
$$

2.5. Fatigue analysis

To evaluate the damage fatigue on the tower, the literature review proposes different solutions. Different standards are presented to evaluate the fatigue, Eurocode3 [21], DNV-GL [22] or DNV-RP-C203 standards [23]. For offshore wind turbine towers, the DNV-RP-C203 standard is the most cited [24], [25], [26]. Other works cite DNV-GL guidelines [27]. The damage of the tower is evaluated using the diagram for steel published by DNV.

The mechanical stress is evaluated in equation (8), Where F_z is the normal force, M_x is the roll moment, M_y is the pitch moment, α is the angular position along the tower base circumference, r is the radius of the tower base, A and J are the area and inertia moment of tower base section.

Table (2) reports the data of the tower base. The data for the material properties are taken from the ontology file [19].

$$\sigma = \frac{F_z}{A} + \frac{M_x}{J} \cdot r \cdot \cos\alpha + \frac{M_y}{J} \cdot r \cdot \sin\alpha \tag{8}$$

Table 2. Geometry properties at the tower base and material properties of steel [19].

Geometry		Material properties	
External diameter	10 m	Yield stress S_y	345 MPa
Internal diameter	9.9210 m	Ultimate load stress S_{ut}	450 MPa
Area A	1.2359 m²		
Inertia J	15.3272 m⁴		

The equation for evaluating the damage equivalent load (DEL) of the tower are described in equations (9, 10, 11, 12,13). DNV reports the equation (9) to link the alternate stress $\Delta\sigma_a$ with the number of cycles, where N^i is the number of cycles to failure with zero mean and constant amplitude (determined experimentally), $\log_{10}\bar{a}$ is the intercept of the curve, m is the slope of the S-N curve. We add the Goodman curve (10) to consider the effect of the mean stress σ_m. The equivalent stress $\Delta\sigma_{eq}$ is computed in equation (11) using the Goodman curve, to be used in equation (12), replacing the original $\Delta\sigma_a$. S_{ut} is the ultimate load stress of the material (450 MPa).

σ_a^i and σ_m^i are the alternate and mean stress of each load cycle evaluated with the Rainflow algorithm, as implemented in Matlab. Finally, the DEL is computed using linear cumulation of damage (Miner method) in equation (13).

$$\log_{10} N^i = \log_{10} \bar{a} - m \log_{10} \Delta\sigma_a^i \tag{9}$$

$$\frac{\sigma_a^i}{\Delta\sigma_{eq}^i} + \frac{\sigma_m^i}{S_{ut}} = 1 \tag{10}$$

$$\Delta\sigma_{eq}^i = \begin{cases} \dfrac{\sigma_a^i S_{ut}}{S_{ut} - \sigma_m^i} & if\ \sigma_m^i > 0 \\ \sigma_a^i & if\ \sigma_m^i \le 0 \end{cases} \tag{11}$$

$$\log_{10} N^i = \log_{10} \bar{a} - m \log_{10} \Delta\sigma_{eq}^i \tag{12}$$

$$DEL = \sum_i^n \frac{1}{N^i} \tag{13}$$

DNV classifies different fatigue curves based on the typology of connection, ranging from non-welded connections, bolted connections, welded connections with parallel direction of the stress and transverse butt welds.

In this work, the tower base is classified as transverse butt weld, welded from both sides (classification D in DNV standard). Table (3) resumes the parameters of the employed bilinear S-N curve.

Table 3. fatigue details of the bilinear goodman diagram of steel from DNV-RP-C203 [23]

Number of cycles	$\log_{10} \bar{a}$	m
For $N \leq 10^7$	12.164	3
For $N > 10^7$	15.606	5

3. Results

In this section, results are compared for different platforms' width. The draft is fixed to 6 meters for all platforms and the centre of mass of the concrete or magnetite pendulum is set to 80 meters under sea water level (figure 1).

The mass of steel used for the main platform is the same for all designs (whether they include a magnetite pendulum, a concrete pendulum, or internal water ballast). The mass of the concrete ballast is larger than the mass of the magnetite ballast, because of the lower density of concrete. Both types of pendulum ballasts are heavier than the steel mass (between 1200-2200 ton), as illustrated in figure (3). A specific design load case is used for time domain analysis. The design load case uses a turbulent wind speed of 11 m/s, corresponding to rated wind speed when the turbine experiences the maximum thrust, a significant wave height of 1.89 meters, and a peak wave period of 6.24 seconds, taken as average of sea condition in Mediterranean Sea for 11 m/s of wind speed.
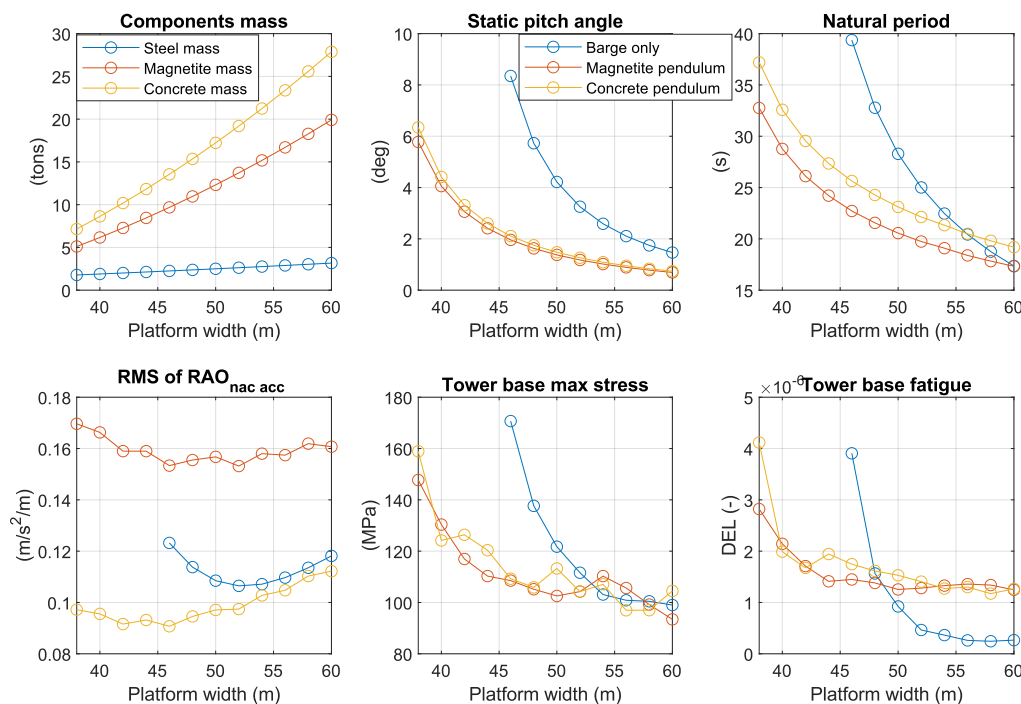

Figure 3. Comparison of different properties among barge only, magnetite and concrete pendulum platforms in function of width.

The waves are codirectional with the wind speed and modelled according to Jonswap spectrum with peak enhancement factor (Gamma) of 1.7, that describes the wave spectrum distribution of energy. Each simulation ran for 22 minutes, discarding the first 2 minutes to avoid transient effects. Figure (3) resumes the results from static analysis, frequency analysis, and time domain analysis. The pitching natural period of the platforms becomes lower with the platform's width, suggesting that the hydrostatic stiffness is predominant respect to pitch inertia for larger widths.

the RMS values for nacelle acceleration in frequency domain are very similar among the different geometries. The concrete pendulum shows the lowest values.
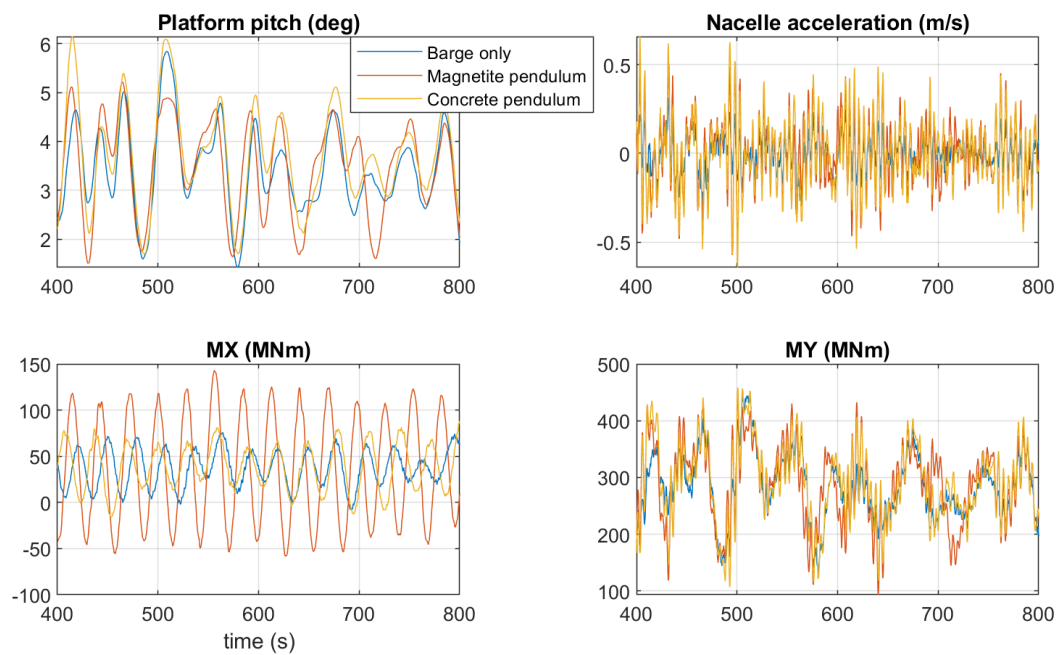

Figure 4. Comparison of pitch motion, nacelle acceleration along x axis and tower base moments for a platform width of 50 meters and 6 meters draft among barge only, concrete pendulum and magnetite pendulum barges.
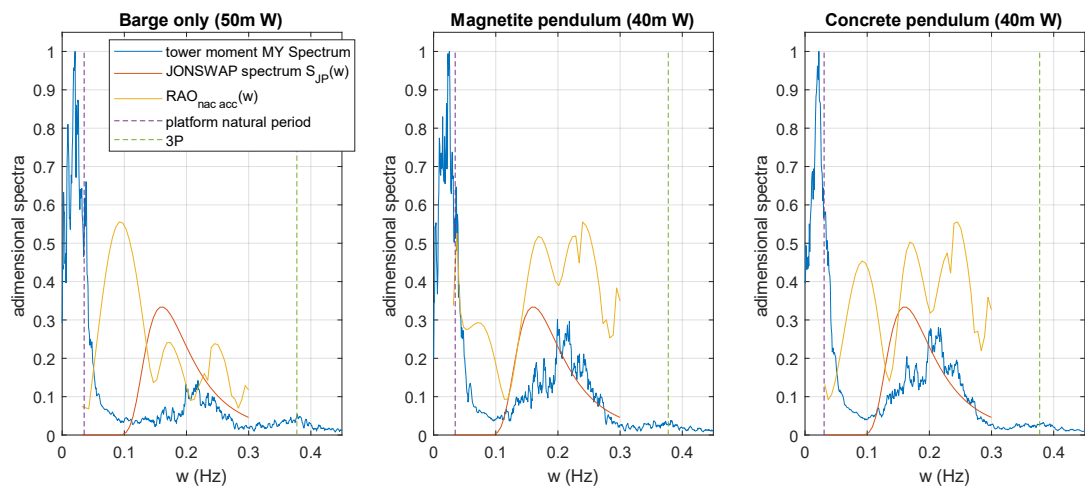

Figure 5. Non-dimensional spectrum of MY moment compared to JONSWAP spectrum, RAO of nacelle acceleration, natural period and 3P (blades pulsation) frequency.

Time domain analysis results show both the maximum stress at the tower base and fatigue damage experience during the load case. The maximum stress is higher for lower static pitch angles due to higher gravitational moment of the rotor nacelle assembly on the tower base.

For the barge-only platform, increasing the platform's width led to a significant reduction in tower base damage until 52 meters width, a trend depicted in figure 3. However, the situation is different for the barge-pendulum configurations. Here, there is no clear minimum DEL. Instead, the DEL remains almost constant for a range of 42-60 meters of width. The barge-only configuration ensures a lower DEL respect to barge pendulum configuration. When comparing the types of ballast used, concrete and magnetite, only a small difference in performance can be noted.

For more detail on time domain analysis results, we can select a variety of quantities to be plotted in time domain and frequency domain (Fast Fourier Transform). Figure 4 shows the comparison between the platform pitch, nacelle acceleration, tower base moment around roll angle (MX) and around pitch angle (MY). The barge-only is a platform with 50 meters of width and for concrete and magnetite pendulum a platform of 40 meters. They share the same value for the static pitch angle (4 degrees). Barge-only and magnetite pendulum have a similar pitch natural period (28 seconds), but concrete pendulum has a higher natural period (32 seconds). Figure 5 shows the non-dimensional spectra of the tower base moment MY, together with the wave (JONSWAP) spectrum and the RAO of the nacelle acceleration ($|w^2 \cdot \xi_{pitch}(w) \cdot h_{hub}|$), the pitching natural period of the platform and the value of 3P, that corresponds to the pulsation due to the passage of the three blades and it is related with the rotor speed. The highest load cycles for the tower base moment MY are caused by the wind and the platform compliance, that generates a high gravitational moment derived from rotor-nacelle assembly weight force.

It can be noted that there is a discrepancy between the intermediate results of rms values of RAO of nacelle acceleration obtained from the frequency domain analysis and time domain results. Frequency domain analysis shows that the concrete-pendulum barge has a lower excitation due to the waves, that is identified as the cause of the higher DEL experienced by the pendulum barge platforms using time domain simulations. This discrepancy needs to be better investigated in future related works.

4. **Conclusion**

The present paper assessed the stability, stress, fatigue of the barge-pendulum configuration using a hydrostatic, frequency and time domain approach. It maintains stability with platform widths ranging from 38 to 46 meters, offering potential advantages in construction and port requirements. However, the design poses challenges in terms of transportation and installation due to its reliance on the pendulum for stability. From preliminary analysis, the fatigue properties of the pendulum-barge are lower than barge-only, determining that the pendulum-barge has not emerged as a solution to mitigate the fatigue damage typically caused by the compliance of the floating device. No significant differences are identified between the concrete and magnetite pendulum. New advancements on this topic may investigate different geometries of the platform, like semisubmersible platforms with pendulum, the relative position of the pendulum and the control system behaviour.

The key points of the study can be summarized as follows:

1. A new methodology for assessing a novel concept of a platform is implemented, based on tower fatigue damage using time domain simulations.
2. The capabilities of MOST for modelling multibody dynamics of a hybrid barge-pendulum platform are demonstrated.
3. the use of a pendulum in place of internal water ballast appears to result in a comparatively poorer performance in terms of fatigue life.
4. The cause of the higher fatigue damage of pendulum barge are attributed to higher nacelle acceleration, caused mainly by the waves.

Reference

[1]   E. Faraggiana, G. Giorgi, M. Sirigu, A. Ghigo, G. Bracco, and G. Mattiazzo, "A review of numerical modelling and optimisation of the floating support structure for offshore wind turbines," *Journal of Ocean Engineering and Marine Energy*, vol. 8, no. 3. Springer Science and Business Media Deutschland GmbH, pp. 433–456, Aug. 01, 2022. doi: 10.1007/s40722-022-00241-2.

[2]   M.-L. Ducasse, C. Colmard, T. Delahaye, F. Vertallier, and S. Rigaud, "OTC-29623-MS Basin Test Validation of New Pendulum Offshore Wind Turbine," 2019. [Online]. Available: http://onepetro.org/OTCONF/proceedings-pdf/19OTC/3-19OTC/D031S033R001/1136216/otc-29623-ms.pdf/1

[3]   E. C. Edwards, A. Holcombe, S. Brown, E. Ransley, M. Hann, and D. Greaves, "Evolution of floating offshore wind platforms: A review of at-sea devices," *Renewable and Sustainable Energy Reviews*, vol. 183. Elsevier Ltd, Sep. 01, 2023. doi: 10.1016/j.rser.2023.113416.

[4]   J. B. Thomsen *et al.*, "Modeling the tetraspar floating offshore wind turbine foundation as a flexible structure in orcaflex and openfast," *Energies (Basel)*, vol. 14, no. 23, Dec. 2021, doi: 10.3390/en14237866.

[5]   T. Choisnet, "Annular buoyant body," US9120542B2, 2015

[6]   E. Gaertner *et al.*, "Definition of the IEA Wind 15-Megawatt Offshore Reference Wind Turbine Technical Report," 2020. [Online]. Available: www.nrel.gov/publications.

[7]   C. Allen *et al.*, "Definition of the UMaine VolturnUS-S Reference Platform Developed for the IEA Wind 15-Megawatt Offshore Reference Wind Turbine Technical Report," 2020. [Online]. Available: www.nrel.gov/publications.

[8]   N. J. Abbas, D. S. Zalkind, L. Pao, and A. Wright, "A Reference Open-Source Controller for Fixed and Floating Offshore Wind Turbines", doi: 10.5194/wes-2021-19.

[9]   E. Faraggiana, M. Sirigu, A. Ghigo, G. Bracco, and G. Mattiazzo, "An efficient optimisation tool for floating offshore wind support structures," *Energy Reports*, vol. 8, pp. 9104–9118, 2022.

[10]   C. Aster, "Salome-Meca." 2018.

[11]   A. Babarit and G. Delhommeau, "Theoretical and numerical aspects of the open source BEM solver NEMOH," in *11th European wave and tidal energy conference (EWTEC2015)*, 2015.

[12]   "Salome 9.9.0," 2024, Accessed: Jan. 17, 2024. [Online]. Available: https://www.salome-platform.org/

[13]   "Orcaflex website. Rope/wire: Minimum breaking loads." Accessed: Dec. 29, 2023. [Online]. Available: https://www.orcina.com/webhelp/OrcaFlex/Content/html/Ropewire,Minimumbreakingloads.htm

[14]   "Orcaflex website. Rope/wire: Axial and bending stiffness." Accessed: Dec. 29, 2023. [Online]. Available: https://www.orcina.com/webhelp/OrcaFlex/Content/html/Ropewire,Axialandbendingstiffness.htm

[15]   "WecSIM theory." Accessed: Mar. 19, 2024. [Online]. Available: https://wec-sim.github.io/WEC-Sim/main/theory/theory.html#irregular-waves

[16]   M. Sirigu, E. Faraggiana, A. Ghigo, and G. Bracco, "Development of MOST, a fast simulation model for optimisation of floating offshore wind turbines in Simscape Multibody," in *Journal of Physics: Conference Series*, Institute of Physics, May 2022. doi: 10.1088/1742-6596/2257/1/012003.

[17]   D. Ogden *et al.*, "Review of WEC-Sim Development and Applications," *International Marine Energy Journal*, vol. 5, no. 3, pp. 293–303, Dec. 2022, doi: 10.36688/imej.5.293-303.

[18]   S. A. Ning, "A simple solution method for the blade element momentum equations with guaranteed convergence," *Wind Energy*, vol. 17, no. 9, pp. 1327–1345, 2014, doi: 10.1002/we.1636.

[19]   "IEA 15 MW RWT." Accessed: Mar. 13, 2024. [Online]. Available: https://github.com/IEAWindTask37/IEA-15-240-RWT

[20]   "6D buoys: Hydrodynamic properties of a rectangular box." Accessed: Nov. 22, 2023. [Online]. Available: https://www.orcina.com/webhelp/OrcaFlex/Content/html/6Dbuoys,Hydrodynamicpropertiesofarectangularbox.htm

[21]   "EN 1993-1-9: Eurocode 3: Design of steel structures - Part 1-9: Fatigue," 2005.

[22]   "DNV-GL guideline".

[23]   DNV GL, "RECOMMENDED PRACTICE DNV GL AS RP-C203: Fatigue design of offshore steel structures," 2014. [Online]. Available: www.dnvgl.com.

[24]　H. Bai, D. Lemosse, Y. Aoues, J. M. Cherfils, and C. Huang, "A probabilistic approach for long-term fatigue analysis of onshore wind turbine tower," in *World Congress in Computational Mechanics and ECCOMAS Congress*, Scipedia S.L., 2021, pp. 1–11. doi: 10.23967/wccm-eccomas.2020.036.

[25]　C. Sun and V. Jahangiri, "Fatigue damage mitigation of offshore wind turbines under real wind and wave conditions," *Eng Struct*, vol. 178, pp. 472–483, Jan. 2019, doi: 10.1016/j.engstruct.2018.10.053.

[26]　Y. Xie, B. Dai, and Z. Huang, "Fatigue life analysis of offshore wind turbine tower under combined action of wind and wave," in *Journal of Physics: Conference Series*, Institute of Physics, 2023. doi: 10.1088/1742-6596/2552/1/012007.

[27]　J. Kim, H. Ahn, B. Seo, and H. Shin, "FATIGUE ANALYSIS AT THE TOWER OF A 12-MW FLOATING OFFSHORE WIND TURBINE," 2018. [Online]. Available: http://asmedigitalcollection.asme.org/OMAE/proceedings-pdf/IOWTC2018/51975/V001T01A043/2506529/v001t01a043-iowtc2018-1064.pdf